Supporting Information

NiCo (oxy)selenide Electrocatalyst via Anionic Regulation for High-performance Lithium-Sulfur Batteries

Yong Li[a], Xuzhen Wang, [a], Minghui Sun[a], Zongbin Zhao[a], Zhiyu Wang[a] and Jieshan*

Qiu[a, b]

a State Key Laboratory of Fine Chemicals, Liaoning Key Laboratory for Energy Materials and Chemical Engineering, School of Chemical Engineering, Dalian University of Technology, Dalian 116024, China.
b College of Chemical Engineering, Beijing University of Chemical Technology, Beijing 100029, China.

*Corresponding authors:
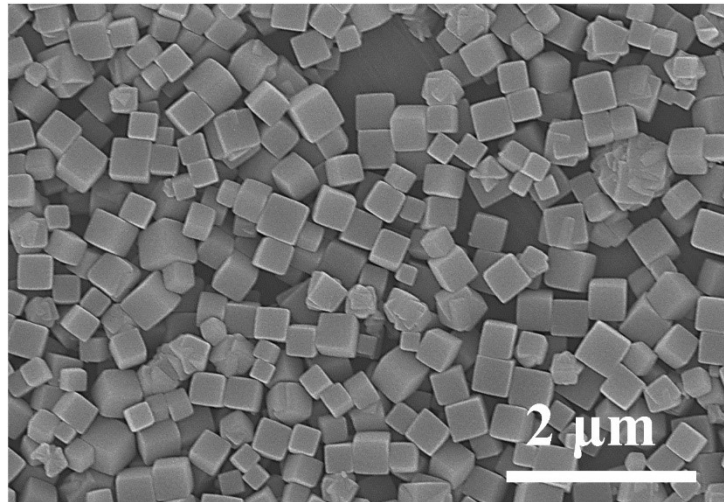 Xuzhen Wang
 E-mail: xzwang@dlut.edu.cn

Fig. S1 SEM image of the cubic ZIF-67 crystals showing the purity and uniformity of the product.
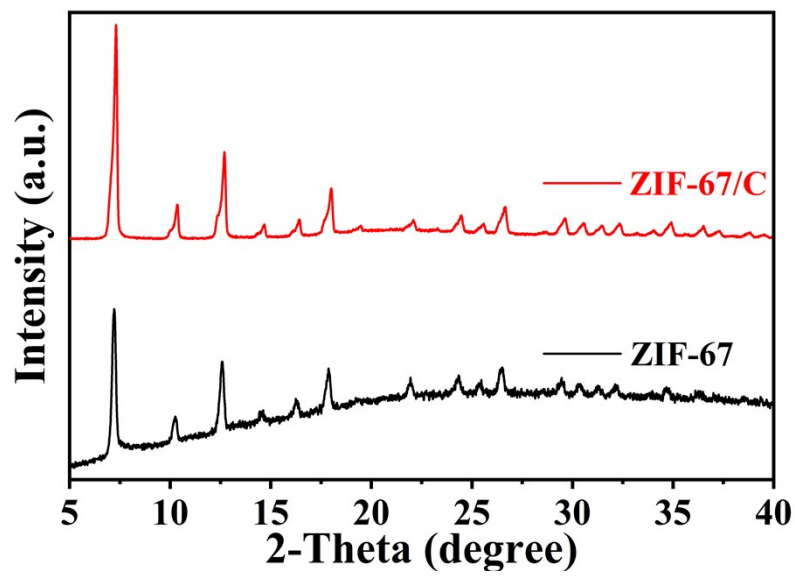

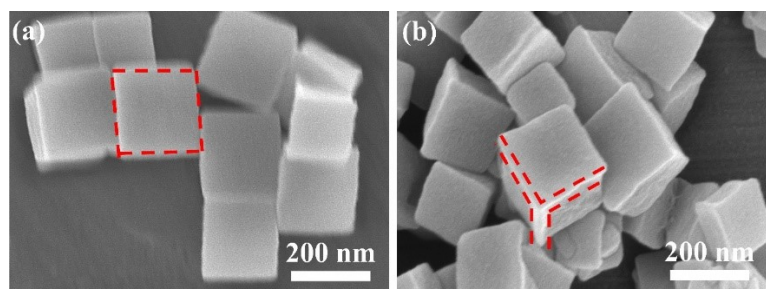**Fig. S2** XRD patterns of ZIF-67 cubes and ZIF-67/C composites.

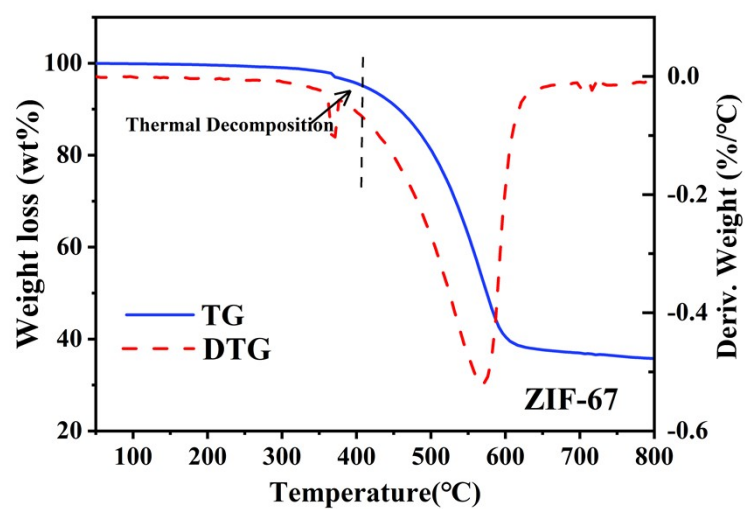**Fig. S3** SEM images of (a) ZIF-67 and (b) ZIF-67/C.

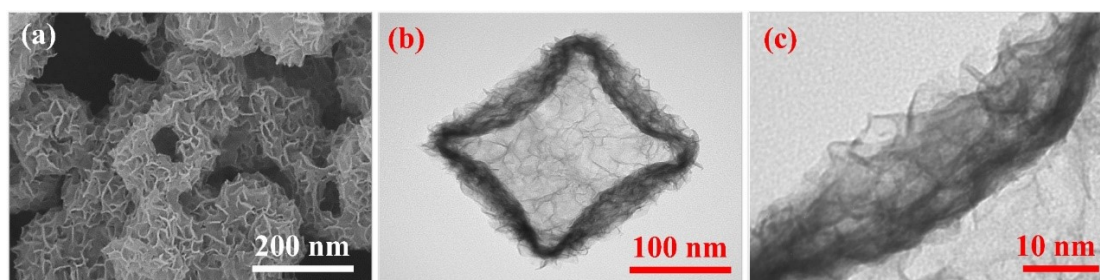**Fig. S4** TGA and DTA curves for ZIF-67.

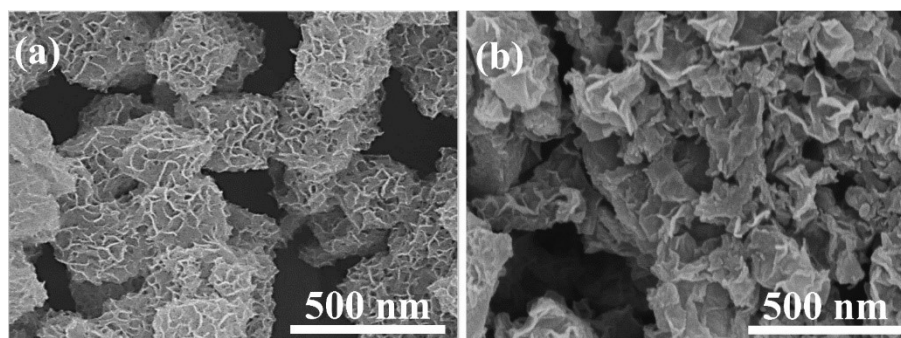**Fig. S5** (a) SEM image and (b, c) TEM images of NiCo-LDH/C.

Fig. S6 SEM images of (a) NiCo-LDH/C and (b) NiCo-LDH.

Fig. S7 Digital photos of various products. From left to right: ZIF-67, ZIF-67/C, NiCo-LDH/C, NiCo-LDH-Se-0, NiCo-LDH-Se-1, NiCo-LDH-Se-2 and NiCo-LDH-Se-4.
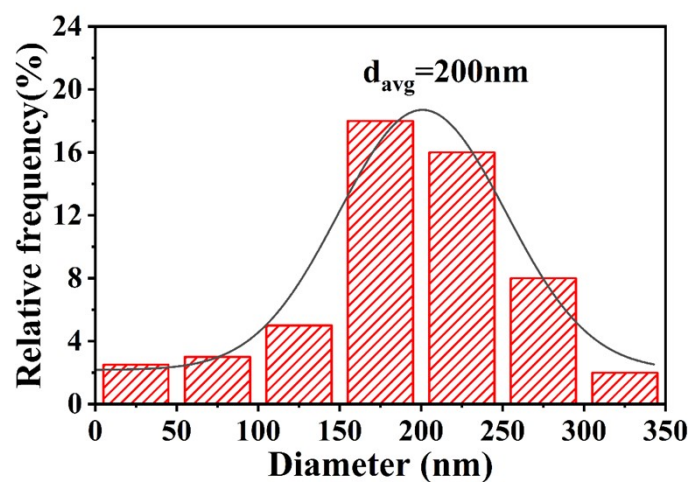

Fig. S8 Histograms showing the size distribution of NiCo-LDH-Se-2.

Table S1 Atomic percentages of the elements in NiCo-LDH-Se-x calculated from XPS survey spectra.

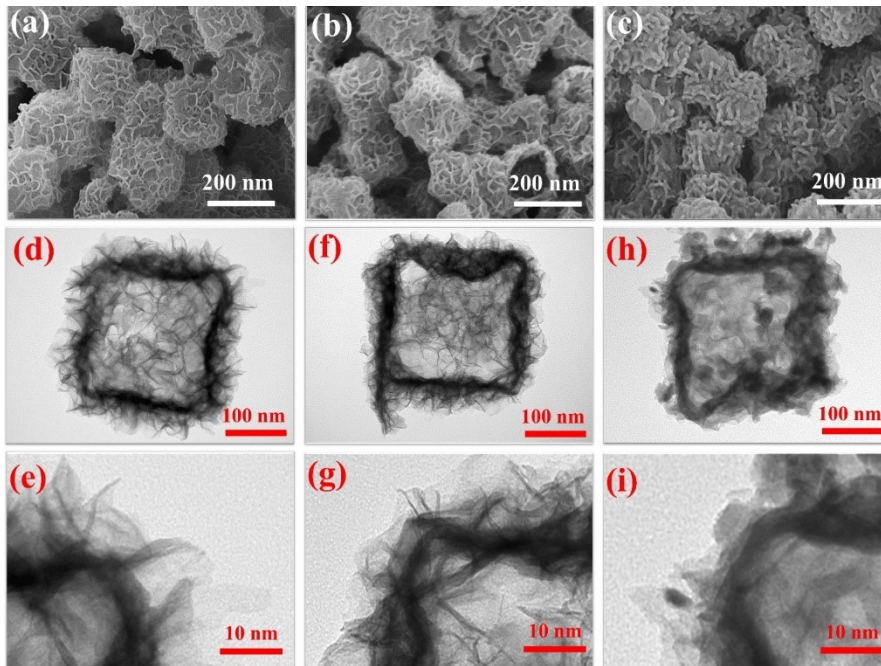| Sample \ Element (at. %)	NiCo-LDH-Se-0	NiCo-LDH-Se-1	NiCo-LDH-Se-2	NiCo-LDH-Se-4
Co	11.3	12.1	11.6	11.1
Ni	24.8	24.3	24.4	21.1.
C	11.5	11.6	10.3	9.8
O	49.0	40.2	37.2	24.6
N	3.4	3.6	3.2	3.2
Se	-	8.2	13.3	30.2

Fig. S9 SEM image of NiCo-LDH-Se-0 (a), NiCo-LDH-Se-1 (b) and NiCo-LDH-Se-4(c). TEM images of NiCo-LDH-Se-0 (d, e), NiCo-LDH-Se-1 (f, g) and NiCo-LDH-Se-4(h, i).
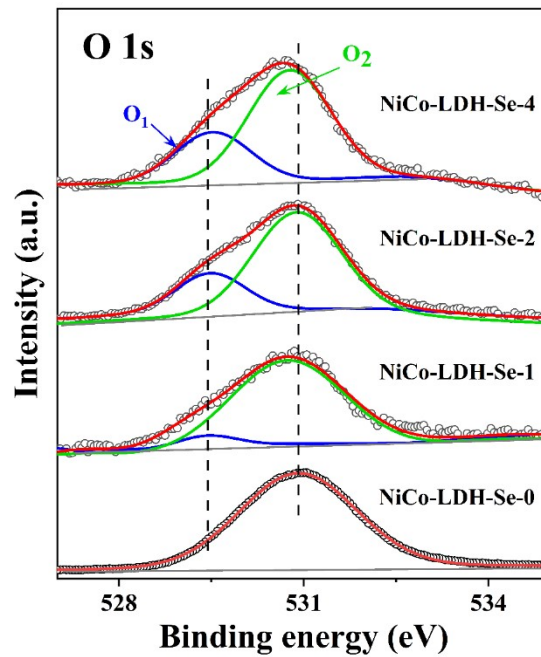

Fig. S10 High resolution O 1s XPS spectra of NiCo-LDH-Se-x electrocatalysts.

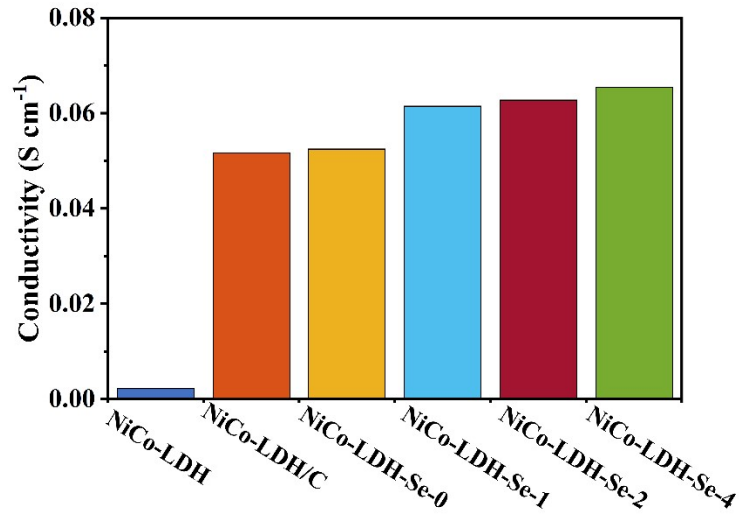**Fig. S11** Electrical conductivity of NiCo-LDH, NiCo-LDH/C and NiCo-LDH-Se-*x*.
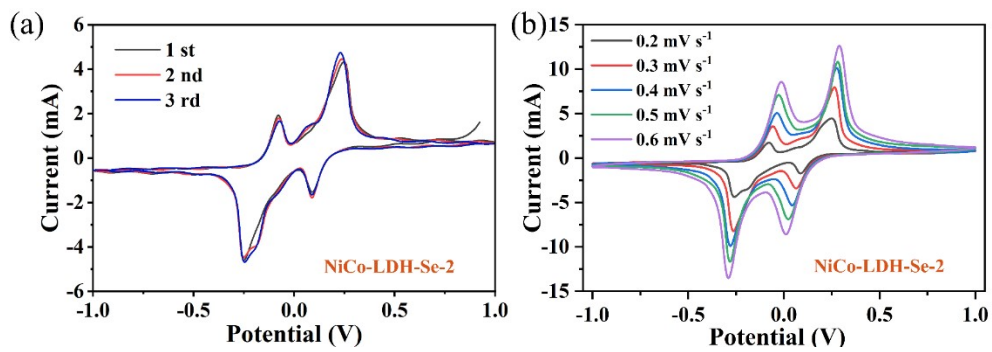

Fig. S12 CV profiles of the symmetric cell with NiCo-LDH-Se-2 electrodes (a) at 0.2 mV s^{-1} and (b) at different current densities.
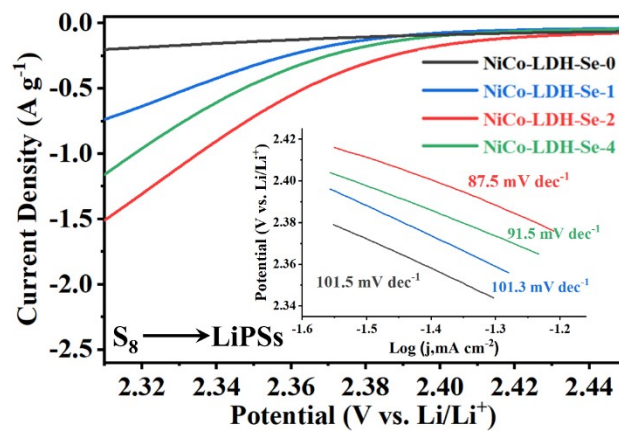

Fig. S13 Potentiostatic polarization curves from the LSV measurements of NiCo-LDH-Se-*x* with the derived Tafel plots as insets on the first reduction processes.

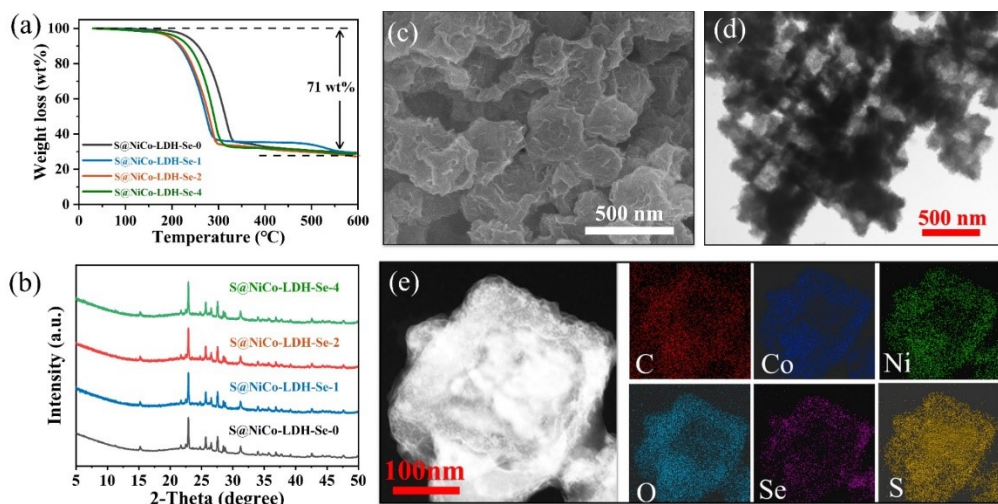**Fig. S14** (a) TGA curves, (b) XRD patterns of S@NiCo-LDH-Se-*x*. (c) SEM image, (d) TEM image, (e) STEM image and the corresponding elemental mappings of S@NiCo-LDH-Se-2 composite.
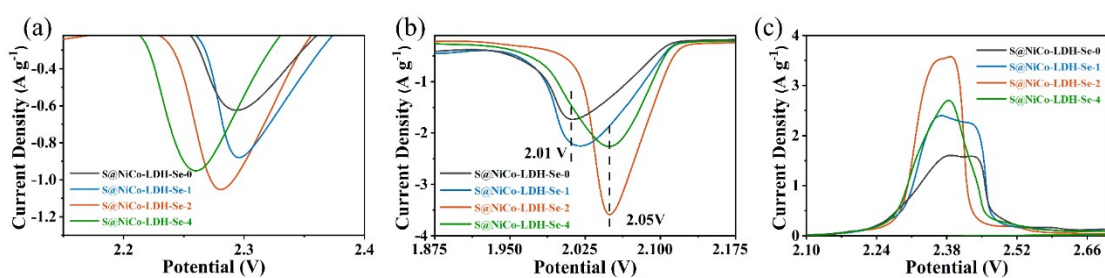

Fig. S15 (a, b) Cathodic peak at 2.3 V (a), 2.05 V (b) and (c) anodic peak of the cell with S@NiCo-LDH-Se-*x*.
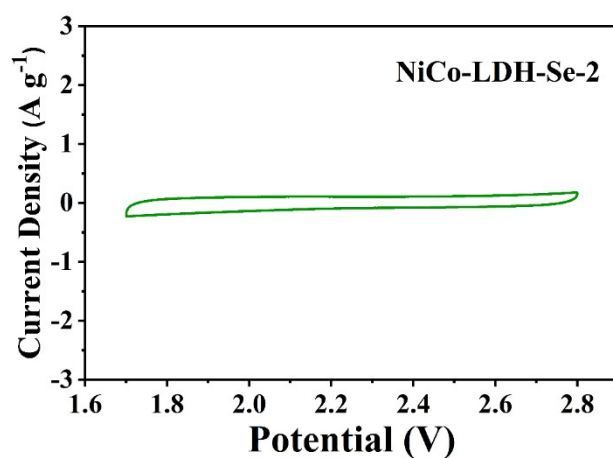
Fig. S16 CV curves of the cell with NiCo-LDH-Se-2 at a scanning rate of 0.1 mV s^{-1} from 2.8 to 1.7 V
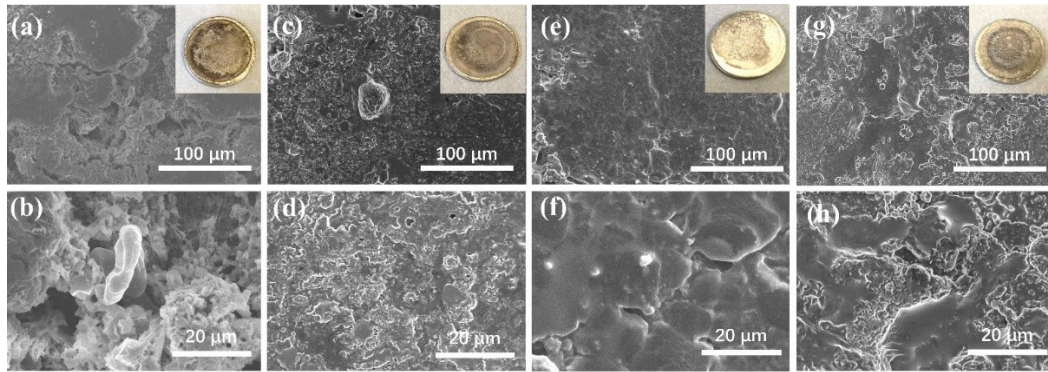
Fig. S17 SEM images and optical photographs of lithium anodes in the cells with (a, b) S@NiCo-LDH-Se-0, (c, d) S@NiCo-LDH-Se-1, (e, f) S@NiCo-LDH-Se-2, and (g, h) S@NiCo-LDH-Se-4 cathodes after 100 cycles at 0.2 C.

Fig. S18 (a) Schematic illustration of chemical adsorption and catalytic effect for polysulfides in S@NiCo-LDH-Se electrode. (b) Performance comparison between S@NiCo-LDH-Se-2 electrode and LDH-basedor CoSe-based cathode materials.

Table S2. Comparison of electrochemical performance of S@NiCo-LDH-Se cathode for Li-S batteries with present state-of-the-art LDH and CoSe-based cathode materials.

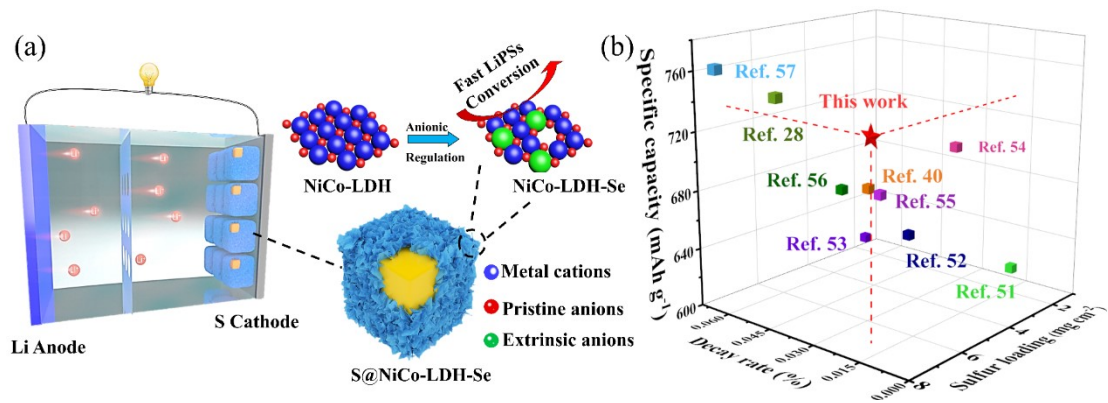| Host material	Capacity (mAh g^{-1}) (Low rate)	Capacity (mAh g^{-1}) (High rate)	Cycling stability (%) (Times, Low rate)	Decay rate (percycle, %) (Times, High rate)	S content (wt.%)
NiCo-LDH-Se (This work)	**1332 (0.2 C)**	**733 (4.0 C)**	**88.1 (100, 0.2 C)**	**0.020 (1000, 2.0 C)**	**71.0**
LDH/Co$_9$S$_8$[40]	1339 (0.1C)	670 (2.0 C)	52.0 (500, 0.1C)	0.047 (1500, 1.0 C)	79.0
LDH/rGo[51]	958 (0.2C)	502 (2.0 C)	60.0 (100, 0.2 C)	0.023 (200, 1.0 C)	64.0
NiCo-LDH@rGO[52]	1336 (0.1 C)	713 (2.0 C)	74.8 (100, 0.1C)	0.030 (800, 2.0 C)	66.0
NiAl@PAB[53]	1216 (0.2C)	614 (3.0 C)	65.0 (200, 0.5 C)	0.133 (300, 1.0 C)	66.0
LDH/S/rGo[54]	1226 (0.2C)	700 (2.0 C)	53.0 (200, 0.2 C)	0.029 (1000, 2.0 C)	61.7
Ni/Fe LDH[55]	1091 (0.2C)	633 (2.0 C)	66.3 (200, 0.1C)	0.041 (1000, 1.0 C)	70.0
CNT-LDH/Ar[56]	1294 (0.1 C)	524 (5.0 C)	87.4 (100, 0.1C)	0.042 (500, 1.0 C)	72.0
CS@HPP[28]	1057 (0.2C)	754 (3.0 C)	83.3 (100, 0.2C)	0.040 (1200, 1.0 C)	72.0
N-CoSe$_2$[57]	1341 (0.2 C)	780 (5.0 C)	68.9 (250, 0.2 C)	0.037 (500, 2.0 C)	70.0

References:

28. Z. Ye, Y. Jiang, L. Li, F. Wu and R. Chen, *Advanced Materials*, 2020, **32**, e2002168.

40. S. Chen, J. Luo, N. Li, X. Han, J. Wang, Q. Deng, Z. Zeng and S. Deng, *Energy Storage Materials*, 2020, **30**, 187-195.

51. F. Xu, C. Dong, B. Jin, H. Li, Z. Wen and Q. Jiang, *Journal of Electroanalytical Chemistry*, 2020, **876**, 114545.

52. W. Qiu, G. Li, D. Luo, Y. Zhang, Y. Zhao, G. Zhou, L. Shui, X. Wang and Z. Chen, *Advanced Science*, 2021, **8**, 2003400.

53. S. Chen, Z. Wu, J. Luo, X. Han, J. Wang, Q. Deng, Z. Zeng and S. Deng, *Electrochimica Acta*, 2019, **312**, 109-118.

54. S. Liu, X. Zhang, S. Wu, X. Chen, X. Yang, W. Yue, J. Lu and W. Zhou, *ACS Nano*, 2020, **14**, 8220-8231.

55. J. Zhang, Z. Li, Y. Chen, S. Gao and X. W. D. Lou, *Angewandte Chemie International Edition*, 2018, **57**, 10944-10948.

56. C. Li, Y. Zhao, Y. Zhang, D. Luo, J. Liu, T. Wang, W. Gao, H. Li and X. Wang, *Chemical Engineering Journal*, 2021, **417**, 129248.

57. M. Wang, L. Fan, X. Sun, B. Guan, B. Jiang, X. Wu, D. Tian, K. Sun, Y. Qiu, X. Yin, Y. Zhang and N. Zhang, ACS Energy Letters, 2020, 5, 3041-3053.